

Article

# Inhibitory Effects of Osthole on Human Breast Cancer Cell Progression via Induction of Cell Cycle Arrest, Mitochondrial Dysfunction, and ER Stress

Wonhyoung Park <sup>1,†</sup>, Sunwoo Park <sup>1,†</sup>, Gwonhwa Song <sup>1,\*</sup>  and Whasun Lim <sup>2,\*</sup>

<sup>1</sup> Department of Biotechnology, Korea University, Seoul 02841, Korea; pwh9224@korea.ac.kr (W.P.); sunwoojump@korea.ac.kr (S.P.)

<sup>2</sup> Department of Food and Nutrition, Kookmin University, Seoul 02707, Korea

\* Correspondence: ghsong@korea.ac.kr (G.S.); wlim@kookmin.ac.kr (W.L.);  
Tel.: +82-2-3290-3012 (G.S.); +82-2-910-4773 (W.L.); Fax: +82-2-3290-4994 (G.S.)

† These authors contributed equally to this work.

Received: 5 August 2019; Accepted: 11 October 2019; Published: 15 November 2019



**Abstract:** Background: Breast cancer is the most commonly diagnosed cancer and the second leading cause of cancer death in women. Although, recently, the number of pathological studies of breast cancer have increased, it is necessary to identify a novel compound that targets multiple signaling pathways involved in breast cancer. Methods: The effects of osthole on cell viability, apoptosis, mitochondria-mediated apoptosis, production of reactive oxygen species (ROS), and endoplasmic reticulum (ER) stress proteins of BT-474 and MCF-7 breast cancer cell lines were investigated. Signal transduction pathways in both cells in response to osthole were determined by western blot analyses. Results: Here, we demonstrated that osthole inhibited cellular proliferation and induced cell cycle arrest through modulation of cell cycle regulatory genes in BT-474 and MCF-7 cells. Additionally, osthole induced loss of mitochondrial membrane potential (MMP), intracellular calcium imbalance, and ER stress. Moreover, osthole induced apoptosis by activating the pro-apoptotic protein, Bax, in both cell lines. Osthole regulated phosphorylation of signaling proteins such as Akt and ERK1/2 in human breast cancer cells. Furthermore, osthole-induced activation of JNK protein-mediated apoptosis in both cell lines. Conclusions: Collectively, the results of the present study indicated that osthole may ameliorate breast cancer and can be a promising therapeutic agent for treatment of breast cancer.

**Keywords:** breast cancer; osthole; apoptosis; MMP depolarization; calcium imbalance; ER stress

## 1. Introduction

Breast cancer is the most common cancer-related cause of mortality in United States [1]. The incidence of breast cancer has risen steadily and is expected to continue to rise [2]. Changing reproductive patterns—pregnancy at later ages and decreased duration of breast feeding promote the acceleration of breast cancer pathogenesis [3]. Breast cancer is frequently diagnosed in advanced stages because few symptoms manifest during the early stages of the disease. Diagnosis and treatment strategies have improved, but numerous barriers to treatment—metastasis, drug side effects, and drug resistance—remain significant challenges [4]. Because of the hypoxic tumor environment, approximately half of patients with advanced breast cancer show resistance to radiotherapy [5]. Additionally, heterogeneity of breast cancer presents a significant obstacle to treatment with specific chemotherapeutic agents [6]. Breast cancer cells could be classified into five subtypes based on gene expression profiles: Luminal A, luminal B, HER2-overexpression, basal, and normal-like. Each subtype shows different clinical outcomes [7]. Particularly, luminal A (MCF-7) and luminal B (BT-474) types

used in this study are ER positive cell lines which are usually hormone responsive. However, BT-474 is a HER2 positive and MCF-7 is a HER2 negative cell line [8]. Moreover, luminal A type has been known to have good prognosis because it is highly differentiated whereas luminal B type has a highly proliferative status and shows poorer prognosis than A type [9]. Therefore, a therapeutic strategy that target these multiple cell types is required.

Phytochemicals exhibit low cytotoxicity to normal cells, but may target heterogeneous cancer cells and multiple signaling pathways [10]. Studies have shown that phytochemicals exert promising therapeutic effects against breast cancer; e.g., curcumin, resveratrol, and sulforaphane-induced apoptosis and cell cycle arrest and decreased proliferation of breast cancer cells [11–13]. Furthermore, studies showed that phytochemicals can target chemo-resistant breast cancer stem cells [14]. Therefore, phytochemicals are considered promising agents for complete treatment of breast cancer.

The biological effects of coumarin and its derivatives have been extensively studied. Studies have shown that the chemical structure of coumarin contributes to its pharmacological properties [15]. Coumarin derivatives have been used as anticoagulants, anti-HIV agents, and for treatment of CNS diseases [16–18]. Osthole (7-methoxy-8-(3-methyl-2-butenyl) coumarin) is a phytochemical from *Cnidium monnieri* (L.) Cusson, which is widely used as a traditional herbal medicine. Osthole is known to exert anti-inflammatory, anti-microbial, and anti-allergic activities [19,20] and has attracted increased attention because of its anti-cancer activity. Osthole is also known to exert therapeutic effects against several cancer types including lung, hepatic, cervical, and ovarian cancer. In addition, osthole induced apoptosis of immortalized hepatocellular carcinoma cells and suppressed hepatic tumor mass growth in mice [21]. Furthermore, osthole inhibited cell proliferation and induced cell cycle arrest in lung and ovarian cancer [22,23]. It exerts anti-cancer effects against breast cancer by attenuating cell proliferation and metastasis [24]. A recent study revealed that osthole suppressed the triple negative breast cancer cell lines by blocking STAT3 signaling pathway [25]. This result supports osthole as having a potential for the management of breast cancer by targeting intracellular signaling pathways. However, the molecular mechanisms of the anticancer effects of osthole in the luminal type of breast cancer cell lines have not been elucidated.

We aimed to examine the anti-cancer mechanisms of osthole in MCF-7 and BT-474 breast cancer cell lines. We evaluated its anti-proliferative apoptotic effects and investigated the disruption of intracellular calcium levels, mitochondrial membrane potential, and ER stress as well as its effects on signaling molecules in the MAPK and PI3K/Akt signaling pathways.

## 2. Materials and Methods

### 2.1. Compounds

Osthole (catalog number: O9265) was purchased from Sigma (St. Louis, MO, USA). Osthole was dissolved in DMSO to prepare a chemical stock for treatment. Antibodies against phosphorylated Akt (Ser<sup>473</sup>, catalog number: 4060), P70S6K (Thr<sup>421</sup>/Ser<sup>424</sup>, catalog number: 9204), S6 (Ser<sup>235</sup>/Ser<sup>236</sup>, catalog number: 2211), ERK1/2 (Thr<sup>202</sup>/Tyr<sup>204</sup>, catalog number: 9101), p90RSK (Thr<sup>573</sup>, catalog number: 9346), JNK (Thr<sup>183</sup>/Tyr<sup>185</sup>, catalog number: 4668), total Akt (catalog number: 9272), P70S6K (catalog number: 9202), S6 (catalog number: 2217), ERK1/2 (catalog number: 4695), p90RSK (catalog number: 9335), JNK (catalog number: 9252), IRE1 $\alpha$  (catalog number: 3294), eIF2 $\alpha$  (catalog number: 5324), Bak (catalog number: 12105S), and Bax (catalog number: 2772) were purchased from Cell Signaling Technology (Beverly, MA, USA). Bcl-xL, p-Bcl-2, cleaved caspase 3 and cleaved caspase 9 were also purchased from Cell Signaling Technology. Antibodies against GRP78 (catalog number: sc-13968), ATF6  $\alpha$  (catalog number: sc-166659), and  $\alpha$ -tubulin (TUBA, catalog number: sc-32293) were purchased from Santa Cruz Biotechnology, Inc (Santa Cruz, CA, USA). Inhibitors of ERK1/2 (U0126, catalog number: E1282) and JNK (SP600125, catalog number: E1305) were purchased from Enzo Life Sciences, Inc (Farmingdale, NY, USA), and a PI3K/Akt inhibitor (LY294002, catalog number: 9901) was purchased from Cell Signaling Technology, Inc.

## 2.2. Cell Culture

BT-474 and MCF-7 cells (breast cancer cells) were purchased from the Korean Cell Line Bank (KCLB; Seoul, Korea) and cultured in RPMI 1640 with HEPES (catalog number: SH30255.01, HyClone, Logan, UT, USA) containing 10% fetal bovine serum. All cells were incubated at 37 °C in a 5% CO<sub>2</sub> atmosphere. For use in experiments, monolayers of BT-474 and MCF-7 cells were grown in culture medium to 70–80% confluence in 100-mm culture dishes. The cells were treated with different doses of osthole with or without cell signaling pathway inhibitors.

## 2.3. Proliferation Assay

Proliferation assays were conducted using a Cell Proliferation ELISA, BrdU kit (catalog number: 11647229001, Roche, Basel, Switzerland) according to the manufacturer's instructions. Briefly, BT-474 and MCF-7 cells ( $1 \times 10^5$  cells per 100  $\mu$ L) were seeded in 96-well plates, then treated with osthole (0, 5, 10, 20, 50, and 100  $\mu$ M). After incubating for 48 h, 10  $\mu$ M bromo-2'-deoxyuridine (BrdU) was added to each well, and the cells were incubated for 2 h at 37 °C. After labeling with BrdU, the cells were fixed and incubated with anti-BrdU-peroxidase (POD) working solution for 90 min. The anti-BrdU-POD bound to BrdU incorporated into newly synthesized cellular DNA, and these immune complexes were detected following reaction with the 3,3',5,5'-tetramethylbenzidine (TMB) substrate. Absorbance of the reaction product was determined at 370 and 492 nm using an ELISA reader. The DMSO-treated group was used as negative control.

## 2.4. Cell Cycle Analysis

Cells ( $1 \times 10^5$  cells per 2 mL) were seeded in 6-well plates, then incubated for 24 h in serum-free RPMI 1640 with HEPES. The cells were then treated with different doses of osthole (0, 10, 20, and 50  $\mu$ M) for 48 h. After treatment, the cells were collected, washed twice with cold 0.1% bovine serum albumin (BSA) in PBS, and fixed with 70% ethanol at 4 °C for 24 h. BT-474 and MCF-7 cells were centrifuged and the supernatant was discarded. Pellets were washed twice with 0.1% BSA-PBS and stained with propidium iodide (PI; BD Biosciences, Franklin Lakes, NJ, USA) and 100  $\mu$ g/mL RNase A (Sigma–Aldrich, St. Louis, MO, USA) for 30 min in the dark. Fluorescence intensity was analyzed using a flow cytometer (BD Biosciences). The DMSO-treated group was used as negative control.

## 2.5. Immunofluorescence Microscopy

The effects of osthole on the expression of proliferating cell nuclear antigen (PCNA) were determined using immunofluorescence microscopy. Cells ( $3 \times 10^4$  cells per 400  $\mu$ L) seeded in confocal dishes were incubated with or without osthole (50  $\mu$ M) for 24 h at 37 °C in a CO<sub>2</sub> incubator. After treatment with osthole, the cells were fixed with methanol for 10 min at –20 °C and then probed with mouse monoclonal PCNA (catalog number: sc-56, Santa Cruz Biotechnology) at a final dilution of 1:100 (2  $\mu$ g/mL). The cells were then incubated with goat anti-mouse IgG Alexa 488 (catalog number: A-11001, Invitrogen, Carlsbad, CA, USA) at a 1:200 dilution for 1 h at room temperature. The cells were then washed using 0.1% bovine serum albumin in phosphate-buffered saline (PBS) and overlaid with 4',6-diamidino-2-phenylindole (DAPI). Images were captured using a LSM710 (Carl Zeiss, Oberkochen, Germany) confocal microscope. The DMSO-treated group was used as negative control.

## 2.6. Annexin V and PI Staining

Osthole-induced apoptosis of breast cancer cells was analyzed using a FITC Annexin V apoptosis detection kit I (BD Biosciences, Franklin Lakes, NJ, USA). The cells ( $1 \times 10^5$  cells per 2 mL) were seeded in 6-well plates and maintained in serum-free medium for 24 h. The cells were then treated with osthole at different doses (0, 10, 20, and 50  $\mu$ M) for 48 h at 37 °C in a CO<sub>2</sub> incubator. The cells were collected by centrifugation, washed with PBS, and resuspended using 1 $\times$  Annexin V binding buffer at  $1 \times 10^6$  cells/mL. Next, 100  $\mu$ L of the cell suspensions ( $1 \times 10^6$  cells) was transferred to 1.5-mL culture

tubes and incubated with 5  $\mu$ L FITC Annexin V and 5  $\mu$ L propidium iodide (PI) for 15 min at room temperature in the dark. Four hundred microliters of 1 $\times$  Annexin V binding buffer was added to the 1.5 mL culture tubes. Fluorescence intensity was determined using a FACS instrument (BD Accuri C6 Plus). The DMSO-treated group was used as negative control.

### 2.7. TUNEL Assay

BT-474 and MCF-7 cells ( $3 \times 10^4$  cells per 400  $\mu$ L) were seeded onto confocal dishes (catalog number:100350, SPL Life Science, Gyeonggi-do, Korea), then treated with osthole at a final concentration of 50  $\mu$ M for 48 h at 37  $^{\circ}$ C in a CO<sub>2</sub> incubator. After incubation, the cells were air-dried and fixed with 4% paraformaldehyde in PBS for 1 h at room temperature. The cells were rinsed with PBS briefly and permeabilized with 0.1% Triton X-100 in 0.1% sodium citrate for 5 min on ice. Next, the cells were subjected to terminal deoxynucleotidyl transferase dUTP nick-end labeling (TUNEL) staining using the In-Situ Cell Death Detection Kit, TMR red for 1 h at 37  $^{\circ}$ C in the dark. The cells were then washed with PBS and counterstained with DAPI (catalog number: D8417, Sigma-Aldrich). Fluorescence was detected using an LSM710 (Carl Zeiss) confocal microscope fitted with a digital microscope AxioCam camera with Zen2009 software. DMSO-treated cells were used as negative control.

### 2.8. JC-1 Mitochondrial Membrane Potential Assay

Changes in MMP were analyzed using a mitochondrial staining kit (catalog number: CS0390, Sigma-Aldrich). Breast cancer cells ( $1 \times 10^5$  cells per 2 mL) were seeded in 6-well plates and treated with osthole at different doses (0, 10, 20, and 50  $\mu$ M) for 48 h at 37  $^{\circ}$ C in a CO<sub>2</sub> incubator. The cells were collected by centrifugation, resuspended in staining solution including 200  $\times$  JC-1 and 1  $\times$  staining buffer, and incubated at 37  $^{\circ}$ C in a CO<sub>2</sub> incubator for 20 min. The stained cells were collected by centrifugation and washed once with 1 $\times$  JC-1 staining buffer. After washing, the cell suspension was centrifuged, and then the cells were resuspended in 500  $\mu$ L of staining buffer. Fluorescence intensity was analyzed using a FACS instrument (BD Accuri C6 Plus). The DMSO-treated group was used as negative control.

### 2.9. Measurement of Cytosolic Calcium Influx

BT-474 and MCF-7 cells ( $1 \times 10^5$  cells per 2 mL) were seeded onto 6-well plates and incubated for 24 h in serum-free medium until the cells reached 70–80% confluence. The cells were treated with different doses of osthole (0, 10, 20, and 50  $\mu$ M) for 48 h at 37  $^{\circ}$ C in a CO<sub>2</sub> incubator. The cells were collected by centrifugation. The collected cells were stained with 3  $\mu$ M fluo-4 AM (Invitrogen) and incubated at 37  $^{\circ}$ C in a CO<sub>2</sub> incubator for 20 min. The stained cells were washed with PBS, and fluorescence intensity was analyzed using a flow cytometer (BD Biosciences). The DMSO-treated group was used as negative control.

### 2.10. Quantitative RT-PCR Analysis

All primers were synthesized by Bioneer (Daejeon, Korea). Each primer was designed using sequences in the GenBank database as illustrated in Table 1. Gene expression levels were measured using a StepOnePlus Real-Time PCR System (Applied Biosystems, Waltham, MA, USA). Sequence-specific products were identified by generating a melting curve. Relative gene expression levels were quantified using the  $2^{-\Delta\Delta CT}$  method. RNA expression in each reaction was normalized to *glyceraldehyde-3-phosphate dehydrogenase (GAPDH)* gene expression. The DMSO-treated samples were used as negative control.

**Table 1.** Primer sequence for quantitative RT-PCR.

Gene Symbol	GenBank No.	Forward Primer (5'→3')	Reverse Primer (5'→3')
CCND1	NM_053056.2	TGCTGGTTTTCTACCCAACG	AGTGCTTGAAATGGAATGG
CCNE1	NM_001238.3 (Updated as NM_001238.4)	CGGCCTTGATCATTCTCG	TCCCCGTCTCCCTTATAACC
CDK2	BT006821.1	TTTGCTGAGATGGTGACTCG	AAGTAACTCCTGGCCACACC
CDK4	NM_000075.3 (Updated as NM_000075.4)	CCGAAGTTCTTCTGCAGTCC	CCACAGAAGAGAGGCTTTCG
CDK6	AK313491.1	CATTCAAAATCTGCCCAACC	TGGAAGTATGGGTGAGACAGG
ER $\alpha$	NM_001328100.2	CAGGCTTGTGGATTTGACC	ATTTCCCTGGTTCCTGTCC
P21	NM_000389.4 (Updated as NM_000389.5)	GACTCTCAGGGTCGAAAACG	GGATTAGGGCTTCTCTTGG
TP53	NM_000546.5	GTCTTTGAACCCCTTGCTTGC	CCACAACAAAACACCAGTGC
FOXO1	NM_002015.3 (Updated as NM_002015.4)	CAGCAAGTTCATTCGTGTGC	CTGTTGTTGTCATGGATGC
GAPDH	NM_001289745.3	GGCTCTCCAGAACATCATCC	TTTCTAGACGGCAGGTCAGG

### 2.11. Western Blot Analyses

Total protein concentration in whole-cell extracts was determined using Bradford reagent (Bio-Rad, Hercules, CA, USA) using BSA as the standard. Proteins were denatured, separated using sodium dodecyl sulfate-polyacrylamide gel electrophoresis (SDS-PAGE), and transferred to nitrocellulose membranes. Blots were developed using enhanced chemiluminescence detection solutions (Super Signal West Pico, Pierce, Rockford, IL, USA) and quantified by measuring the intensity of light emitted from correctly sized bands under UV light using a Chemi Doc EQ system and Quantity One software (Bio-Rad). Immunoreactive proteins were detected using specific antibodies against phosphorylated and total proteins at a 1:1000 dilution. Total protein or  $\alpha$ -tubulin (TUBA) was used to normalize the levels of target proteins. The signal intensity in each dose was represented as the relative value compared to signal intensity in 0  $\mu$ M.

### 2.12. Statistical Analysis

All quantitative data was subjected to least squares analysis of variance (ANOVA) using the General Linear Model procedure of Statistical Analysis System software (SAS Institute, Inc., Cary, NC, USA). All significance tests were performed using the appropriate error terms according to the expectation of the mean squares for error. A  $p$ -value less than or equal to 0.05 was considered statistically significant. Data are presented as least-square means (LSMs) with standard errors (SEs).

## 3. Results

### 3.1. Osthole Selectively Inhibited Cellular Proliferation of Human Breast Cancer Cells

To investigate the effect of osthole on breast cancer cells, a proliferation assay was performed with BT-474 and MCF-7 cells. Osthole reduced cell proliferation in a dose-dependent manner (Figure 1A). Osthole decreased proliferation of BT-474 cells by 51% ( $p < 0.01$ ) at 50  $\mu$ M and 59% ( $p < 0.001$ ) at 100  $\mu$ M. Proliferation of MCF-7 cells was decreased by 54% ( $p < 0.01$ ) following 50  $\mu$ M osthole treatment and 70% ( $p < 0.001$ ) following 100  $\mu$ M osthole treatment. However, osthole did not affect the cell viability of MCF-12A normal breast epithelial cells (Figure 1B). Based on the results of the proliferation assay, all subsequent experiments were performed using 50  $\mu$ M osthole. Next, we evaluated the expression of a proliferative marker in breast cancer cells following osthole treatment (Figure 1C,D).

Green fluorescent signal associated with PCNA was reduced following osthole treatment in BT-474 (33%) and MCF-7 (39%) cells. To examine the effects of osthole on the cell cycle progression in breast cancer cells, we analyzed cell cycle distribution by monitoring DNA content of BT-474 and MCF-7 cells. The percentages of cells occupying each cell cycle phase were calculated compared with DMSO treated cells. Osthole increased the number of cells at sub-G1 phase 2.3-fold in BT-474 cells (Figure 1E). In MCF-7 cells, osthole increased the number of G1 phase cells and reduced the number of sub-G1 and S phase cells (Figure 1F).

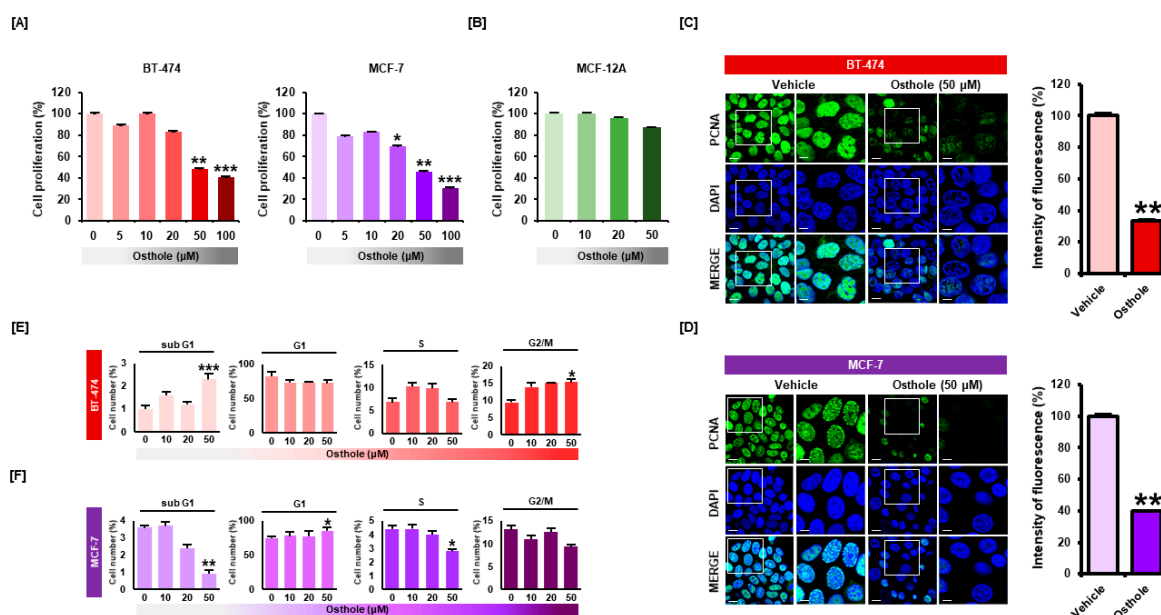


**Figure 1.** Osthole inhibited cell proliferation in human breast cancer cells. (A) Proliferation of breast cancer cells was analyzed using cell proliferation assays. Osthole (0, 5, 10, 20, 50, and 100 μM) decreased the proliferation of BT-474 and MCF-7 cells in a dose-dependent manner. (B) Effect of osthole on MCF-12A normal mammary epithelial cell proliferation in a dose dependent manner (0, 10, 20, and 50 μM). (C,D) Proliferative cell nuclear antigen (PCNA) was detected using immunofluorescence analysis. The green signal associated with PCNA was attenuated in osthole-treated cells compared to vehicle-treated cells. Nuclei were counterstained with DAPI (blue). The graph shows the intensity of PCNA fluorescence. (E,F) Regulatory effect of osthole on cell cycle progression in breast cancer cells. The number of cells in each cell cycle phase was analyzed by propidium iodide (PI) staining of DNA contents using flow cytometry. All experiments were performed in biological triplicate and the asterisks represent statistically significant differences compared to control (DMSO-treated cells; 0 μM) (\*  $p < 0.05$ , \*\*  $p < 0.01$  and \*\*\*  $p < 0.001$ ).

### 3.2. Osthole Downregulated Gene Expression Associated with Cell Cycle Progression in Breast Cancer Cells

We investigated the mRNA expression of cell cycle-related genes—*Cyclin*, *CDK*, *forkhead box protein O1* (*FOXO1*), *P21*, *TP53*, and *ERα*. The expression of *Cyclin D1* (Figure 2A), *Cyclin E1* (Figure 2B), *CDK2* (Figure 2C), and *CDK6* (Figure 2E) were significantly decreased following treatment with 50 μM osthole in BT-474 and MCF-7 cells. The mRNA expression of *CDK4* was decreased only in BT-474 cells (Figure 2D). *Estrogen receptor α* (*ERα*), a key effector in breast cancer progression, was decreased approximately 0.5-fold ( $p < 0.001$ ) and 0.2-fold ( $p < 0.001$ ) in BT-474 and MCF-7 cells, respectively (Figure 2F). The CDK inhibitor *CDKN1A* (also known as *P21*), and transcription factors associated with cell cycle arrest including *TP53* and *FOXO1*, were elevated following osthole treatment in MCF-7 cells (Figure 2G–I). Similarly, osthole increased the expression of *P21* and *TP53* in BT-474 cells without affecting *FOXO1* expression. These findings suggested that osthole induced cell cycle arrest by modulating gene expression of cell cycle regulators in two different cell types of breast cancer cell lines.

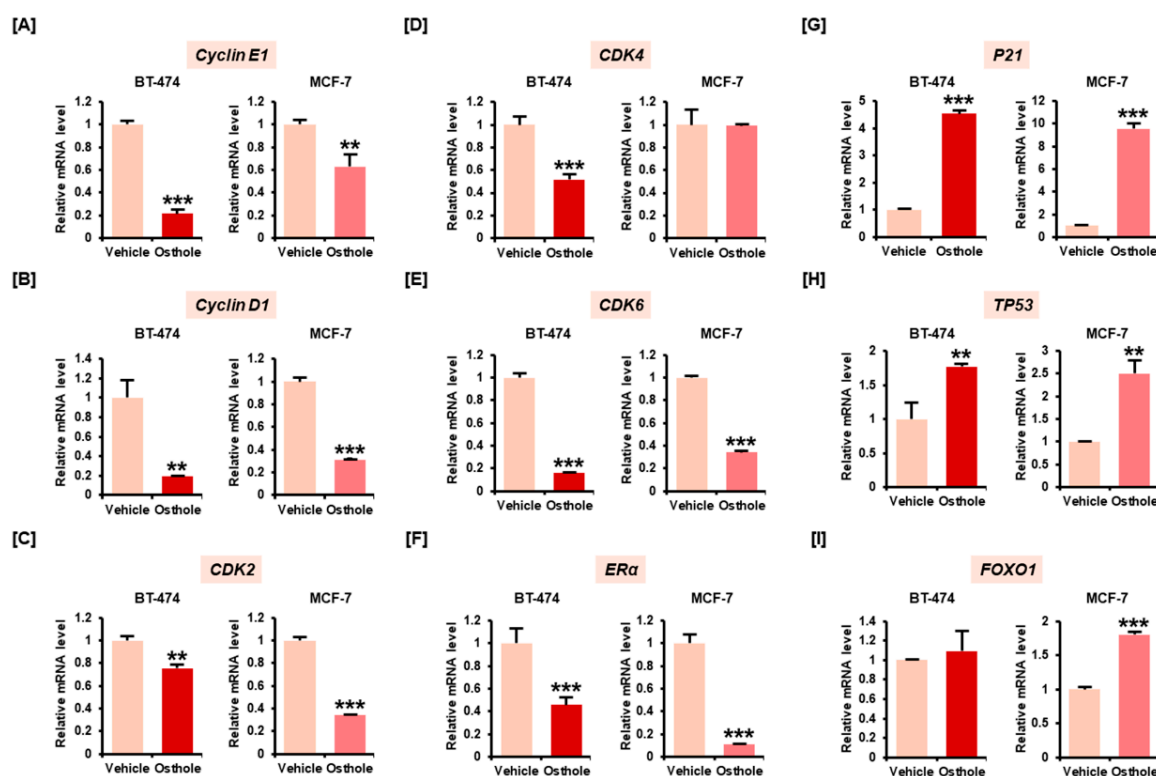


**Figure 2.** Relative mRNA expression of cell cycle-related genes including *cyclin E1* (A), *cyclin D1* (B), *CDK2* (C), *CDK4* (D), *CDK6* (E), *ERα* (F), *P21* (G), *TP53* (H), and *FOXO1* (I). Expression of cell cycle-related genes in breast cancer cell lines was analyzed by quantitative RT-PCR using cDNA templates based on RNA isolated from BT-474 and MCF-7 cells. The graphs indicate the relative mRNA expression in breast cancer cell lines treated with vehicle and osthole for 24 h. All experiments were performed in technical triplicate and the asterisks represent statistically significant differences compared to vehicle-treated cells (\*\*  $p < 0.01$  and \*\*\*  $p < 0.001$ ).

### 3.3. Osthole Disrupted the Mitochondrial Membrane Potential and Intracellular Calcium Flux in Human Breast Cancer Cells

To determine the effects of osthole on intracellular homeostasis in breast cancer cells, we investigated changes in mitochondrial membrane potential (MMP) using the JC-1 assay. The green signal associated with JC-1 monomer was increased in a dose-dependent manner to 9300% ( $p < 0.001$ ) in BT-474 cells and 1212% ( $p < 0.001$ ) in MCF-7 cells, which showed that osthole induced depolarization of the mitochondria membrane in breast cancer cells (Figure 3A,B). Furthermore, osthole gradually increased cytosolic calcium influx in both cell lines (Figure 3C,D). Cytosolic calcium levels increased to 174% ( $p < 0.01$ ) in BT-474 cells and 156% ( $p < 0.05$ ) in MCF-7 cells in response to 50  $\mu\text{M}$  osthole treatment.

### 3.4. Osthole Activated ER Stress Pathways in Human Breast Cancer Cells

Due to the finding that osthole disrupted intracellular calcium homeostasis in breast cancer cells, we measured the effect of osthole on the endoplasmic reticulum (ER) using western blot analysis. Osthole upregulated the expression of ER stress-inducing proteins in a dose-dependent manner in BT-474 and MCF-7 cells. The expression of GRP78 was increased by approximately 7-fold ( $p < 0.001$ ) in both cell lines (Figure 4A). Additionally, the expression of IRE1 $\alpha$ , cleaved ATF6 $\alpha$ , and phospho-eIF2 $\alpha$  increased by 2.5-fold, 3-fold, and 1.7-fold, respectively, following treatment with 50  $\mu\text{M}$  osthole (Figure 4B–D). These results showed that osthole induced ER stress in human breast cancer cells.

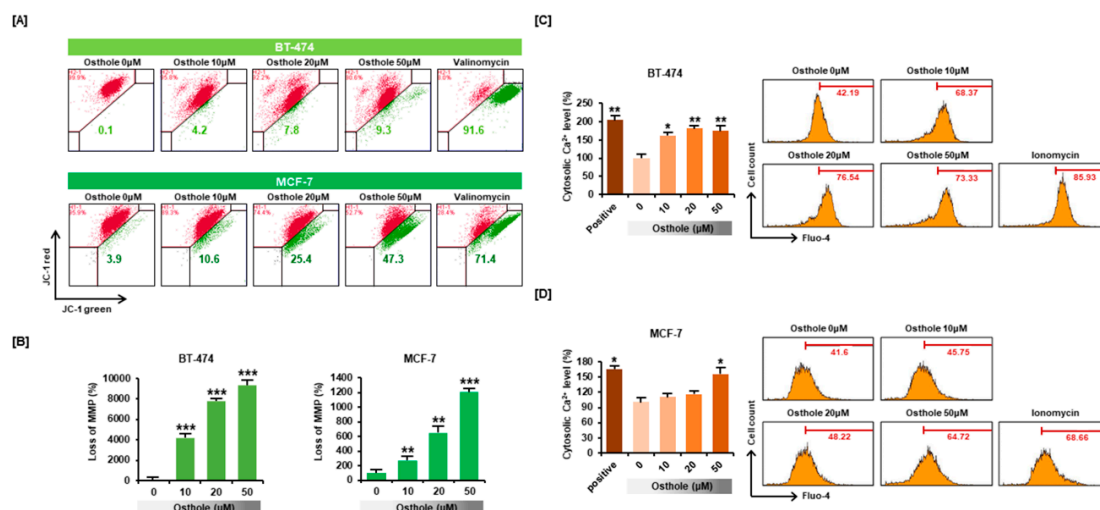


**Figure 3.** Effects of osthole on mitochondrial dysfunction and cytosolic calcium influx in human breast cancer cells. (A,B) Mitochondrial membrane potential (MMP) was evaluated in JC-1 stained BT-474 and MCF-7 cells using flow cytometry. Depolarization of mitochondria was indicated by increased green fluorescence in the dot plot. The cells treated with Valinomycin (1 μg/mL) for 20 min were used as a positive control for mitochondrial depolarization. (C,D) Calcium levels in the cytoplasm were evaluated using the cytosolic calcium indicator, Fluo-4. The cells treated with Ionomycin (12 μM) for 5 min were used as a positive control for calcium flux. All experiments were performed in biological triplicate and the asterisks represent statistically significant differences compared to vehicle-treated cells (\*  $p < 0.05$ , \*\*  $p < 0.01$  and \*\*\*  $p < 0.001$ ).

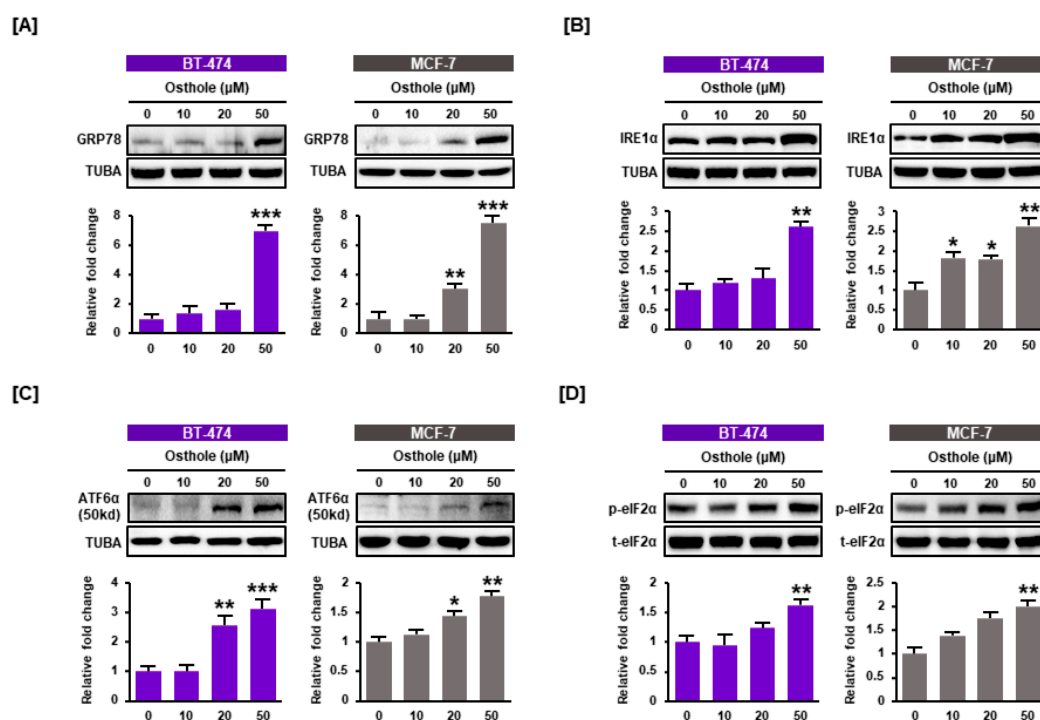


**Figure 4.** ER stress induced by osthole treatment in human breast cancer cells. The levels of the ER regulatory proteins GRP78 (A), IRE1α (B), ATF6α (C), and eIF2α (D) were analyzed using western blot analysis of BT-474 and MCF-7 cells. The levels of GRP78, IRE1α, and ATF6α were normalized to α-tubulin (TUBA), and phosphor eIF2α was normalized to total eIF2α protein. All experiments were performed in biological triplicate and the asterisks represent statistically significant differences (\*  $p < 0.05$ , \*\*  $p < 0.01$  and \*\*\*  $p < 0.001$ ).



### 3.5. Osthole Induced Apoptosis in Human Breast Cancer Cells

We examined whether osthole induced apoptosis in human breast cancer cells using the Annexin V assay. The number of apoptotic cells increased in an osthole dose-dependent manner to 423% ( $p < 0.001$ ) in BT-474 cells and 186% ( $p < 0.01$ ) in MCF-7 cells (Figure 5A,B). Furthermore, the expression of pro-apoptotic proteins was analyzed using western blot analysis. Osthole treatment resulted in increased the expression of Bax about 2-fold in both cell lines ( $p < 0.001$ ). Contrastingly, Bak was only slightly increased in response to osthole treatment in both breast cancer cells (Figure 5C,D). Moreover, cleaved form of caspase 3 was also increased about 2.6-fold and 1.5-fold in BT-474 and MCF-7 cells. Cleaved caspase 9 was increased by 2.8-fold in MCF-7 whereas not significantly changed in BT-474 cells. Additionally, we investigated the expression of Bcl-xL and phosphorylated Bcl-2 known as antiapoptotic factors. Osthole decreased the expression of Bcl-xL less than 0.63-fold and 0.38-fold in BT-474 and MCF-7 cells. Phosphorylated Bcl-2 was decreased less than 0.56-fold in MCF-7 cells while p-Bcl-2 in BT-474 has not been changed.

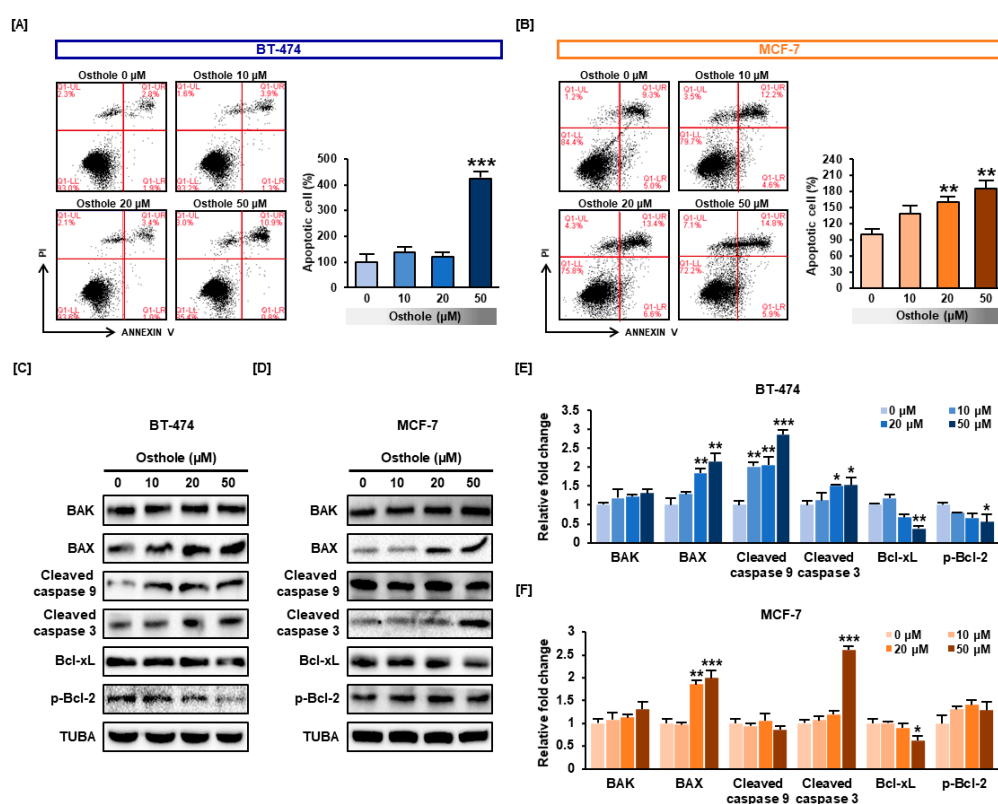


**Figure 5.** The apoptotic effects of osthole on human breast cancer cells. (A,B) Apoptotic cells were detected by flow cytometry using Annexin V/PI staining. The graph represents increased numbers of cells in the late apoptotic phase (upper right side of dot plot) in response to osthole (0, 10, 20, and 50 μM). Data were analyzed relative to the DMSO control (0 μM). (C,D) The expressions of the pro-apoptotic proteins including Bax, Bak, cleaved caspase 3 and cleaved caspase 9, and anti-apoptotic proteins including Bcl-xL and p-Bcl-2 were analyzed by western blot in BT-474 and MCF-7 cells. The expression levels of apoptotic proteins in BT-474 (E) and MCF-7 (F) were represented as bar graphs. The expression levels of proteins were normalized to  $\alpha$ -tubulin (TUBA). All experiments were performed in biological triplicate and the asterisks indicate statistically significant differences compared to control (DMSO-treated cells; 0 μM) (\*  $p < 0.05$ , \*\*  $p < 0.01$  and \*\*\*  $p < 0.001$ ).

### 3.6. Osthole Regulated the PI3K/Akt and MAPK Signaling Pathways in Human Breast Cancer Cells

To determine osthole-mediated cell signaling mechanisms, phosphorylation of signaling proteins associated with the PI3K/Akt and MAPK pathways was detected by western blotting. Osthole

inhibited the phosphorylation of Akt, p70S6K, and S6 in BT-474 cells (Figure 6A), but upregulated phosphorylation of these proteins in MCF-7 cells (Figure 6B). Similarly, phosphorylated ERK1/2 was decreased in BT-474 cells, but increased in MCF-7 cells. Contrastingly, phosphorylated P90RSK and JNK were increased in response to osthole in BT-474 and MCF-7 cells.

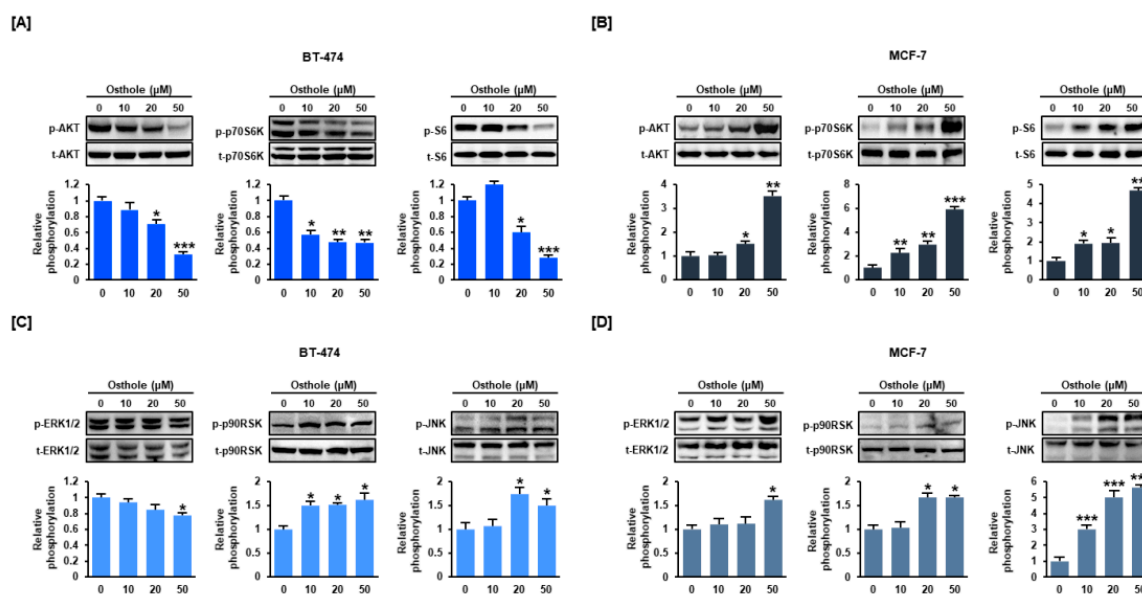


**Figure 6.** Effect of osthole on phosphorylation of PI3K/Akt and MAPK pathway proteins in human breast cancer cells. The levels of Akt, p70S6K, S6 (A,B), ERK1/2, p90RSK, and JNK (C,D) were detected by western blot analysis. Each phosphorylated protein was normalized to the corresponding total protein. Band intensity is shown in the graph as relative value compared to non-treated control (0  $\mu\text{M}$ ). All experiments were performed in biological triplicate and the asterisks indicate statistically significant differences (\*  $p < 0.05$ , \*\*  $p < 0.01$  and \*\*\*  $p < 0.001$ ).

### 3.7. Interaction between Osthole-Mediated Modulation of the PI3K/Akt and MAPK Pathways

Modulation of the PI3K/Akt and MAPK pathways by osthole was verified by pretreatment with pharmacological inhibitors including LY294002 (PI3K inhibitor, 20  $\mu\text{M}$ ), U0126 (ERK1/2 inhibitor, 10  $\mu\text{M}$ ), and SP600125 (JNK inhibitor, 20  $\mu\text{M}$ ). Phosphorylation of Akt, p70S6K, and S6 was completely inhibited by LY294002 and U0126 in BT-474 cells (Figure 7A). Increased Akt activation was inhibited only by LY294002. However, phosphorylation of P70S6K and S6 was blocked by LY294002 and U0126 in MCF-7 cells (Figure 7B). U0126 inhibited the phosphorylation of ERK1/2 in BT-474 and MCF-7 cells. Additionally, phosphorylation of ERK1/2 was increased by SP600125 in BT-474 cells. Moreover, phosphorylation of JNK was blocked by SP600125 and decreased by LY294002 in MCF-7 cells (Figure 7C,D).

### 3.8. Combinational Effects of Osthole with Commercial Chemotherapeutic Drugs

We investigated the anti-cancer effects of combination treatment with osthole and the commercial anticancer drug, paclitaxel, in breast cancer cells using the Annexin V assay. In BT-474 cells, treatment with paclitaxel increased the number of apoptotic cells by 377% and 456% at 5  $\mu\text{M}$  and 10  $\mu\text{M}$  concentrations, respectively. However, combined treatment with osthole (50  $\mu\text{M}$ ) increased apoptosis by 418% and 569% at each concentration of paclitaxel ( $p < 0.001$ ) (Figure 8A). In MCF-7 cells, paclitaxel increased the number of apoptotic cells by 114% and 117% at 5  $\mu\text{M}$  and 10  $\mu\text{M}$  concentrations, whereas combined treatment with osthole increased the apoptosis of MCF-7 cells by 199% ( $p < 0.01$ ) and 265% ( $p < 0.001$ ), respectively (Figure 8B). These results showed that the combinational treatment exerted higher apoptotic effect than treatment with osthole or paclitaxel alone in breast cancer cell lines.

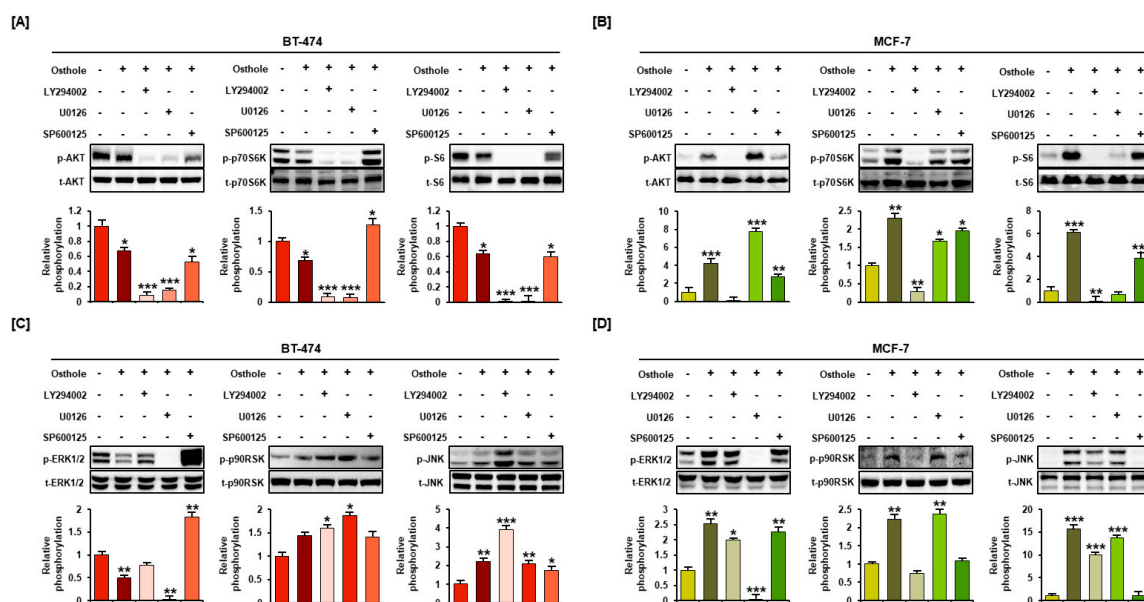


**Figure 7.** Combinational effect of pharmacological inhibitors on osthole-mediated signaling pathways in human breast cancer cells. After incubation with LY294002 (Akt inhibitor), U0126 (ERK1/2 inhibitor), and SP600125 (JNK inhibitor) for 2 h, BT-474 and MCF-7 cells were treated with 50  $\mu$ M osthole for 1 h. Changes in phosphorylation of Akt, p70S6K, S6 (A,B), ERK1/2, p90RSK, and JNK (C,D) were analyzed by western blotting. The graph shows relative phosphorylation of each protein compared to that in non-treated control (0  $\mu$ M). All experiments were performed in biological triplicate and the asterisks indicate statistically significant differences compared to non-treated control (\*  $p < 0.05$ , \*\*  $p < 0.01$  and \*\*\*  $p < 0.001$ ).

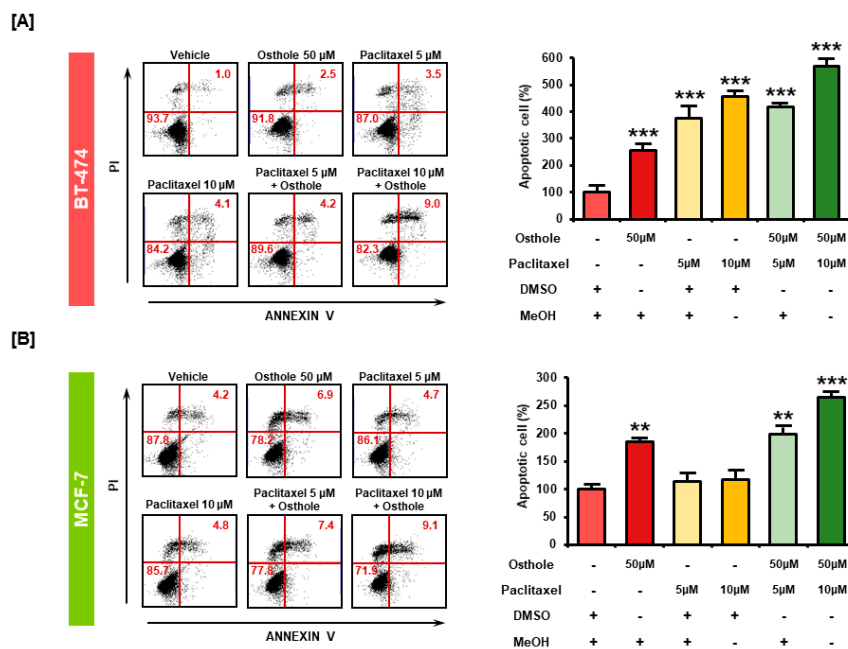


**Figure 8.** Combinational apoptotic effect of osthole and conventional chemotherapeutic agents. The proportion of apoptotic cells following treatment with osthole with and without paclitaxel was detected using Annexin V/PI staining in BT-474 (A) and MCF-7 (B). BT-474 and MCF-7 cells were incubated with osthole, paclitaxel, or a combination of both for 48 h. Data are represented in the graph as the percentage of apoptotic cells compared with vehicle-treated control (100%). All experiments were performed in biological triplicate and the asterisks indicate statistically significant differences compared to Vehicle-treated control (\*\*  $p < 0.01$  and \*\*\*  $p < 0.001$ ).

#### 4. Discussion

We showed that osthole exerted anti-cancer effects against BT-474 and MCF-7 human breast cancer cell lines. It induced cell cycle arrest and suppressed cell proliferation. Osthole disrupted intracellular homeostasis by depolarizing the mitochondrial membrane potential and increasing cytosolic calcium levels. Moreover, osthole activated ER stress proteins and regulated the activity of the PI3K/Akt and MAPK signaling pathways, resulting in apoptosis of breast cancer cells (Figure 9).

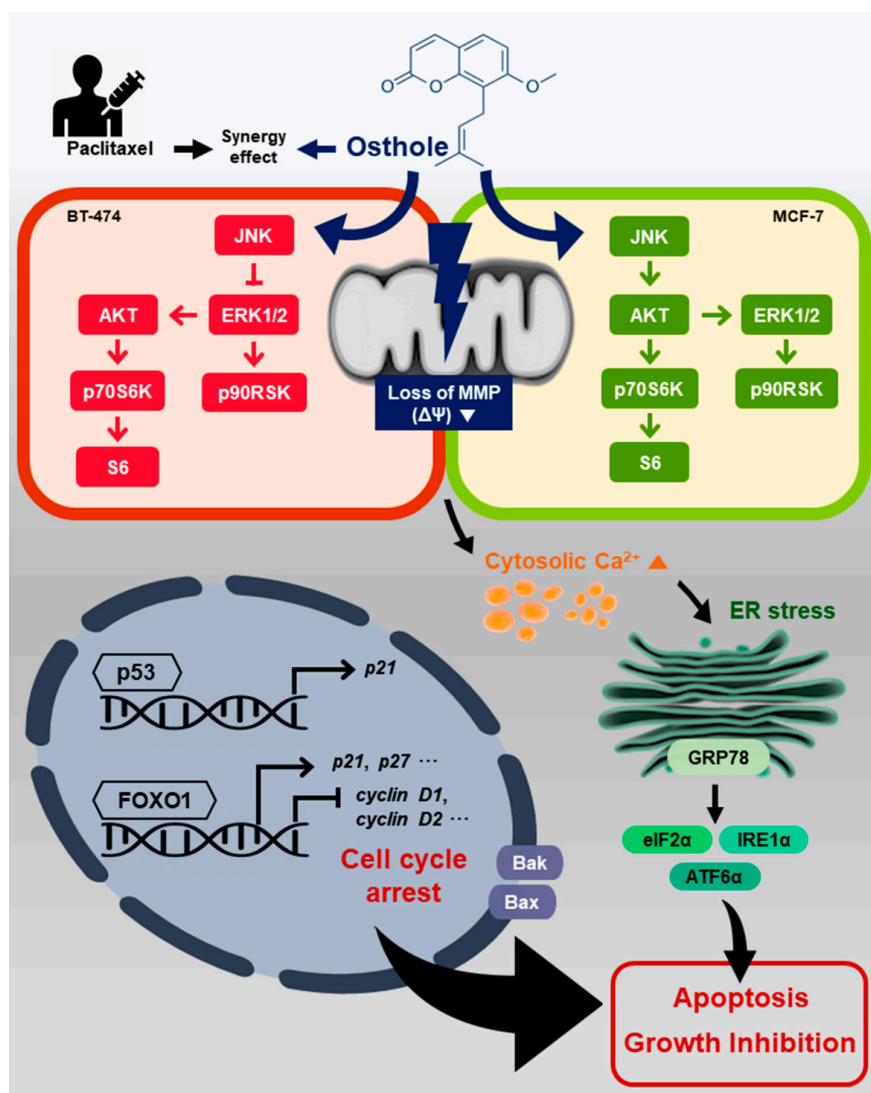


**Figure 9.** Hypothetical mechanism of action of osthole in human breast cancer cell lines. Osthole induced loss of the MMP and increased cytoplasmic calcium levels. ER stress-response proteins and pro-apoptotic proteins were increased in BT-474 and MCF-7 cells. Osthole upregulated JNK in both cell lines, downregulated the Akt and ERK1/2 signaling pathways in BT-474 cells, and upregulated these pathways in MCF-7 cells. Osthole induced growth inhibition and apoptosis in breast cancer cell lines.

Breast cancer, the most commonly diagnosed cancer and the second leading cause of cancer death in women, is comprised of a heterogeneous population of cells. Clinical subtypes of breast cancer are classified based on gene expression profiles [26]. Each breast cancer subtype responds differently to anti-cancer treatments [27]. Recently, molecular classification of breast cancer has been used for treatment design, resulting in improved survival rates [28]. Although, recently, the number of pathological studies of breast cancer have increased, several challenges including heterogeneity, gene

mutation, and tumor microenvironment remain [29]. Particularly, tumor heterogeneity complicates the treatment of breast cancer. Therefore, it is necessary to identify a novel compound that targets multiple signaling pathways involved in breast cancer.

Natural extracts—*Ganoderma lucidum* extract, luteolin, and ginsenoside—are known to exert anti-cancer effects in human breast cancer cell lines [30–32]. Apigenin also inhibited cell growth and increased the number of BT-474 cells in the sub-G1 phase [33]. Studies showed that osthole inhibited cell proliferation, migration, and invasion of breast cancer cells [24]. Similarly, here, osthole inhibited cell proliferation and induced apoptosis in both breast cancer cell lines evaluated. Additionally, osthole induced sub-G1 phase arrest in BT-474 cells and G1 phase arrest in MCF-7 cells.

The cell cycle is regulated by protein complexes consisting of cyclin and cyclin-dependent kinase (CDK). In many cancers, cell cycle arrest has been considered a potential target for cancer therapies. Reduction of cyclin D inhibited tumor growth and induced cell death in esophageal, colon, and pancreatic cancer [34–36]. Furthermore, targeting cyclin E1 induced cell cycle arrest and apoptosis in breast cancer cells [37] and hepatocellular carcinoma cells [38]. Additionally, various anti-cancer agents exert medicinal effects by reducing the expression of CDK family proteins; e.g., flavopiridol induced cell cycle arrest through inhibition of CDKs in human breast cancer cells [39], and CYC202, a potent inhibitor of CDK2, reduced tumor growth in vitro and in vivo [40]. Likewise, here, osthole inhibited the mRNA expression of *cyclin E1*, *cyclin D1*, *CDK2*, and *CDK6* in BT-474 and MCF-7 cell lines. Furthermore, osthole suppressed the mRNA expression of *ER $\alpha$* , which plays a critical role in breast cancer progression in both cell lines. *ER $\alpha$*  was shown to directly bind to TP53 and downregulate transcriptional activation of TP53 and functional genes in the p53-mediated apoptotic pathway [41,42]. In response to DNA damage, TP53 was activated and facilitated the transcription of downstream genes including *P21* [43]. *P21* is a CDK inhibitor that binds to multiple CDK/cyclin complexes and PCNA [44]. The mRNA expression of *P21* is also increased by FOXOs, which are localized in the nucleus and act as transcription factors [45]. Quercetin increased FOXO1 expression, resulting in induction of *P21*, leading to cell cycle arrest and apoptosis in oral cancer [46]. Here, osthole upregulated the mRNA expression of *TP53*, *P21*, and *FOXO1*, resulting in cell cycle arrest and apoptosis in human breast cancer cell lines.

Mitochondria-dependent apoptosis is a major apoptotic pathway in mammalian cells. Osthole induced apoptosis via disruption of the mitochondrial membrane potential in cholangiocarcinoma [47]. Additionally, osthole induced mitochondrial permeability transition, resulting in apoptosis in human hepatocarcinoma cells [48]. Disruption of the mitochondrial membrane activated pro-apoptotic proteins—Bak and Bax—in the outer membrane, resulting in proteolipid pore formation. Cytochrome c was secreted into the cytoplasm through these pores, resulting in enhanced caspase activity [49]. Similarly to previous studies, osthole depolarized the mitochondrial membrane and increased Bax, Bak, and activity of caspase 3 and 9 in BT-474 and MCF-7 cells in our study. Thus, we concluded that osthole induces apoptosis in breast cancer cells via activation of proapoptotic factors including caspases proteins. Recent studies revealed that activation of caspase proteins could generate proteolytically-activated proapoptotic fragments [50–52]. Therefore, further research on other apoptotic pathways will contribute to understanding osthole-mediated cell death mechanisms in breast cancer cells.

Calcium signaling is involved in various cellular functions including cell proliferation and apoptotic cell death [53]. Furthermore, disruption of intracellular calcium homeostasis can induce endoplasmic reticulum (ER) stress, leading to the unfolded protein response (UPR) [54]. Osthole has been shown to activate the ER stress signaling pathway in osteoblasts [55]. Similarly, we showed that the ER stress signaling proteins GRP78, IRE1 $\alpha$ , ATF6 $\alpha$ , and phosphorylated eIF2 $\alpha$  were upregulated by osthole in BT-474 and MCF-7 cells. These results indicated that osthole disrupted the mitochondrial membrane potential (MMP) and calcium homeostasis, resulting in ER stress in human breast cancer cell lines.

Abnormal cell proliferation and invasion induced by alterations of signaling pathways are hallmarks of cancer [56]. The PI3K/Akt and MAPK/ERK1/2 signaling pathways are important in normal cellular physiology, and are common targets for treatment of diverse human cancers, including breast

cancer [57]. Particularly, the PI3K/Akt signaling pathway plays an important role in cell proliferation, growth, and survival in cancer [58]. Therefore, the PI3K/Akt pathway is constitutively activated in several types of cancer cells; e.g., the HER2 receptor family activates the PI3K/Akt signaling pathway and leads to sustained proliferative signaling in breast cancer cells [59]. Osthole was shown to inhibit the Akt signaling pathway and induce apoptosis in HER2-overexpressing breast cancer cells [60]. Furthermore, osthole suppressed proliferation and induced apoptotic cell death via inhibition of the PI3K/Akt and ERK1/2 signaling pathways in rat glioma cells [61]. Similarly, here, osthole downregulated the phosphorylation of Akt, p70S6K, S6, and ERK1/2 in BT-474 cells.

In contrast to the results obtained using BT-474 cells, osthole activated the Akt and ERK1/2 pathways in MCF-7 cells. In contrast to the known cell proliferative properties of PI3K/Akt, Akt facilitated apoptosis rather than cell growth under pathologic conditions; e.g., rapamycin, a cytotoxic chemotherapeutic agent, induced cancer cell death via activation of Akt [62]. Reduced Akt was shown to confer resistance to oxidative stress and cellular apoptosis [63]. Similarly, the ERK signaling pathway promotes apoptosis in cell type- and stimulus-dependent manners [64]. Several phytochemicals—baicalein and kaempferol—enhanced apoptosis by activating the ERK1/2 pathway in MCF-7 cells [65]. Moreover, doxorubicin activated ERK1/2 and induced G1 phase cell cycle arrest and apoptosis in MCF-7 cells [66]. Additionally, JNK activation mediated apoptotic signaling through upregulation of pro-apoptotic genes and caspase activity [67]. In breast cancer, tocotrienol and rotenone induced apoptosis via activation of JNK [68,69]. Here, osthole increased JNK phosphorylation in both breast cancer cell lines.

The effects of combination treatment with osthole and LY294002, U0126, or SP600125 was evaluated in both breast cancer cell lines. Phosphorylation of Akt, p70S6K, and S6 was strongly suppressed by the PI3K inhibitor and by the MEK inhibitor. The ERK1/2 pathway was activated by the JNK inhibitor in BT-474. These results indicated that ERK1/2 was inhibited by JNK, and activated the Akt pathway in BT-474 cells. In MCF-7 cells, the Akt pathway was downregulated by the JNK inhibitor and ERK1/2, p90RSK, and JNK were downregulated by the PI3K inhibitor. These results suggested that osthole-induced JNK activation increased PI3K/Akt and ERK1/2 signaling, resulting in apoptosis.

The signaling discrepancies between the two breast cancer cell lines might be associated with distinctive molecular profile including receptor status [70]. Indeed, BT-474 and MCF-7 cells have been known to exert different clinical responses to the same treatment [71]. Therefore, further validation of basal activity on two major pathways and the status of receptors associated with signaling cascade should be conducted to understand the differences between the BT-474 and MCF-7 cells.

## 5. Conclusions

We demonstrated the anti-cancer effects of osthole in human breast cancer cells. Osthole inhibited cell proliferation via reduced PCNA expression and induced cell cycle arrest. It downregulated the mRNA expression of cell cycle regulators—cyclin and CDK family proteins—and upregulated the mRNA expression of *P21*, *TP53*, and *FOXO1* transcription factor. Additionally, osthole induced apoptotic cell death by disrupting the MMP and increasing intracellular calcium levels and ER stress in human breast cancer cells. Osthole also modulated the PI3K/Akt and MAPK/ERK1/2 signaling pathways. Moreover, the apoptotic cell death by paclitaxel was increased with cotreatment with osthole. Thus, osthole has great potential in human breast cancer therapy.

**Author Contributions:** The authors' responsibilities were as follows: G.S. and W.L. conceived and designed the culture experiments, the cell culture methodology, and other all experiments; W.P. and S.P. collected experimental samples and conducted all experiments; W.P., S.P., G.S., and W.L. analysed and interpreted the data and contributed to the development of the manuscript. All authors contributed to its critical review and agreed on the final version.

**Funding:** This research was supported by a grant of the Korea Health Technology R&D Project through the Korea Health Industry Development Institute, funded by the Ministry of Health and Welfare [grant number: HI17C0929], and the National Research Foundation of Korea (NRF) grant, funded by the Ministry of Science and ICT(MSIT) [grant number: 2018R1C1B6009048].

**Acknowledgments:** We would like to thank School of Life Sciences and Biotechnology for BK21 PLUS, Korea University for supporting the publication fee

**Conflicts of Interest:** The authors declare no conflict of interest.

## References

1. Siegel, R.L.; Miller, K.D.; Jemal, A. Cancer statistics, 2018. *CA A Cancer J. Clin.* **2018**, *68*, 7–30. [[CrossRef](#)]
2. Winters, S.; Martin, C.; Murphy, D.; Shokar, N.K. Breast Cancer Epidemiology, Prevention, and Screening. *Prog. Mol. Biol. Transl. Sci.* **2017**, *151*, 1–32. [[CrossRef](#)] [[PubMed](#)]
3. Winters, S.; Martin, C.; Murphy, D.; Shokar, N.K. Chapter One—Breast Cancer Epidemiology, Prevention, and Screening. In *Progress in Molecular Biology and Translational Science*; Lakshmanaswamy, R., Ed.; Academic Press: Cambridge, MA, USA, 2017; Volume 151, pp. 1–32.
4. Redig, A.J.; McAllister, S.S. Breast cancer as a systemic disease: A view of metastasis. *J. Intern. Med.* **2013**, *274*, 113–126. [[CrossRef](#)] [[PubMed](#)]
5. Sinha, D.; Sarkar, N.; Biswas, J.; Bishayee, A. Resveratrol for breast cancer prevention and therapy: Preclinical evidence and molecular mechanisms. In *Seminars in Cancer Biology*; Academic Press: Cambridge, MA, USA, 2016; Volume 40, pp. 209–232. [[CrossRef](#)]
6. Rattani, N.S.; Swift-Scanlan, T. Deconstructing breast cancer heterogeneity: Clinical implications for women with Basal-like tumors. *Oncol. Nurs. Forum* **2014**, *41*, 639–646. [[CrossRef](#)] [[PubMed](#)]
7. Sorlie, T.; Perou, C.M.; Tibshirani, R.; Aas, T.; Geisler, S.; Johnsen, H.; Hastie, T.; Eisen, M.B.; van de Rijn, M.; Jeffrey, S.S.; et al. Gene expression patterns of breast carcinomas distinguish tumor subclasses with clinical implications. *Proc. Natl. Acad. Sci. USA* **2001**, *98*, 10869–10874. [[CrossRef](#)] [[PubMed](#)]
8. Holliday, D.L.; Speirs, V. Choosing the right cell line for breast cancer research. *Breast Cancer Res.* **2011**, *13*, 215. [[CrossRef](#)]
9. Subik, K.; Lee, J.-F.; Baxter, L.; Strzepak, T.; Costello, D.; Crowley, P.; Xing, L.; Hung, M.-C.; Bonfiglio, T.; Hicks, D.G.; et al. The Expression Patterns of ER, PR, HER2, CK5/6, EGFR, Ki-67 and AR by Immunohistochemical Analysis in Breast Cancer Cell Lines. *Breast Cancer (Auckl.)* **2010**, *4*, 35–41. [[CrossRef](#)]
10. Dandawate, P.R.; Subramaniam, D.; Jensen, R.A.; Anant, S. Targeting cancer stem cells and signaling pathways by phytochemicals: Novel approach for breast cancer therapy. *Semin. Cancer Biol.* **2016**, *40*, 192–208. [[CrossRef](#)]
11. Kanematsu, S.; Uehara, N.; Miki, H.; Yoshizawa, K.; Kawanaka, A.; Yuri, T.; Tsubura, A. Autophagy inhibition enhances sulforaphane-induced apoptosis in human breast cancer cells. *Anticancer Res.* **2010**, *30*, 3381–3390.
12. Garvin, S.; Öllinger, K.; Dabrosin, C. Resveratrol induces apoptosis and inhibits angiogenesis in human breast cancer xenografts in vivo. *Cancer Lett.* **2006**, *231*, 113–122. [[CrossRef](#)]
13. Koohpar, Z.K.; Entezari, M.; Movafagh, A.; Hashemi, M. Anticancer activity of curcumin on human breast adenocarcinoma: Role of Mcl-1 gene. *Iran. J. Cancer Prev.* **2015**, *8*, e2331. [[CrossRef](#)] [[PubMed](#)]
14. Kim, S.-H.; Sehrawat, A.; Singh, S.V. Dietary chemopreventative benzyl isothiocyanate inhibits breast cancer stem cells in vitro and in vivo. *Cancer Prev. Res.* **2013**, *6*, 782–790. [[CrossRef](#)] [[PubMed](#)]
15. Hoult, J.R.; Paya, M. Pharmacological and biochemical actions of simple coumarins: Natural products with therapeutic potential. *Gen. Pharmacol.* **1996**, *27*, 713–722. [[CrossRef](#)]
16. Skalicka-Woźniak, K.; Orhan, I.E.; Cordell, G.A.; Nabavi, S.M.; Budzyńska, B. Implication of coumarins towards central nervous system disorders. *Pharmacol. Res.* **2016**, *103*, 188–203. [[CrossRef](#)] [[PubMed](#)]
17. Holbrook, A.M.; Pereira, J.A.; Labiris, R.; McDonald, H.; Douketis, J.D.; Crowther, M.; Wells, P.S. Systematic overview of warfarin and its drug and food interactions. *Arch. Intern. Med.* **2005**, *165*, 1095–1106. [[CrossRef](#)]
18. Yu, D.; Suzuki, M.; Xie, L.; Morris-Natschke, S.L.; Lee, K.H. Recent progress in the development of coumarin derivatives as potent anti-HIV agents. *Med. Res. Rev.* **2003**, *23*, 322–345. [[CrossRef](#)]
19. Okamoto, T.; Yoshida, S.; Kobayashi, T.; Okabe, S. Inhibition of concanavalin A-induced mice hepatitis by coumarin derivatives. *Jpn. J. Pharmacol.* **2001**, *85*, 95–97. [[CrossRef](#)]
20. Matsuda, H.; Tomohiro, N.; Ido, Y.; Kubo, M. Anti-allergic effects of *Cnidium monnieri* fructus (dried fruits of *Cnidium monnieri*) and its major component, osthole. *Biol. Pharm. Bull.* **2002**, *25*, 809–812. [[CrossRef](#)]
21. Zhang, L.; Jiang, G.; Yao, F.; He, Y.; Liang, G.; Zhang, Y.; Hu, B.; Wu, Y.; Li, Y.; Liu, H. Growth inhibition and apoptosis induced by osthole, a natural coumarin, in hepatocellular carcinoma. *PLoS ONE* **2012**, *7*, e37865. [[CrossRef](#)]

22. Xu, X.; Zhang, Y.; Qu, D.; Jiang, T.; Li, S. Osthole induces G2/M arrest and apoptosis in lung cancer A549 cells by modulating PI3K/Akt pathway. *J. Exp. Clin. Cancer Res.* **2011**, *30*, 33. [[CrossRef](#)]
23. Jiang, G.; Liu, J.; Ren, B.; Tang, Y.; Owusu, L.; Li, M.; Zhang, J.; Liu, L.; Li, W. Anti-tumor effects of osthole on ovarian cancer cells in vitro. *J. Ethnopharmacol.* **2016**, *193*, 368–376. [[CrossRef](#)] [[PubMed](#)]
24. Yang, D.; Gu, T.; Wang, T.; Tang, Q.; Ma, C. Effects of osthole on migration and invasion in breast cancer cells. *Biosci. Biotechnol. Biochem.* **2010**, *74*, 1430–1434. [[CrossRef](#)] [[PubMed](#)]
25. Dai, X.; Yin, C.; Zhang, Y.; Guo, G.; Zhao, C.; Wang, O.; Xiang, Y.; Zhang, X.; Liang, G. Osthole inhibits triple negative breast cancer cells by suppressing STAT3. *J. Exp. Clin. Cancer Res.* **2018**, *37*, 322. [[CrossRef](#)] [[PubMed](#)]
26. Santa-Maria, C.A.; Gradishar, W.J. Changing treatment paradigms in metastatic breast cancer: Lessons learned. *JAMA Oncol.* **2015**, *1*, 528–534. [[CrossRef](#)] [[PubMed](#)]
27. López-Otín, C.; Diamandis, E.P. Breast and prostate cancer: An analysis of common epidemiological, genetic, and biochemical features. *Endocr. Rev.* **1998**, *19*, 365–396. [[CrossRef](#)] [[PubMed](#)]
28. Perez, E.A. Breast cancer management: Opportunities and barriers to an individualized approach. *Oncologist* **2011**, *16*, 20–22. [[CrossRef](#)]
29. Polyak, K. Heterogeneity in breast cancer. *J. Clin. Investig.* **2011**, *121*, 3786–3788. [[CrossRef](#)]
30. Hu, H.; Ahn, N.-S.; Yang, X.; Lee, Y.-S.; Kang, K.-S. Ganoderma lucidum extract induces cell cycle arrest and apoptosis in MCF-7 human breast cancer cell. *Int. J. Cancer* **2002**, *102*, 250–253. [[CrossRef](#)]
31. Kang, J.H.; Song, K.H.; Woo, J.K.; Park, M.H.; Rhee, M.H.; Choi, C.; Oh, S.H. Ginsenoside Rp1 from Panax ginseng exhibits anti-cancer activity by down-regulation of the IGF-1R/Akt pathway in breast cancer cells. *Plant Foods Hum. Nutr.* **2011**, *66*, 298–305. [[CrossRef](#)]
32. Park, S.H.; Ham, S.; Kwon, T.H.; Kim, M.S.; Lee, D.H.; Kang, J.W.; Oh, S.R.; Yoon, D.Y. Luteolin induces cell cycle arrest and apoptosis through extrinsic and intrinsic signaling pathways in MCF-7 breast cancer cells. *J. Env. Pathol. Toxicol. Oncol.* **2014**, *33*, 219–231. [[CrossRef](#)]
33. Seo, H.S.; Jo, J.K.; Ku, J.M.; Choi, H.S.; Choi, Y.K.; Woo, J.K.; Kim, H.I.; Kang, S.Y.; Lee, K.M.; Nam, K.W.; et al. Induction of caspase-dependent extrinsic apoptosis by apigenin through inhibition of signal transducer and activator of transcription 3 (STAT3) signalling in HER2-overexpressing BT-474 breast cancer cells. *Biosci. Rep.* **2015**, *35*. [[CrossRef](#)] [[PubMed](#)]
34. Arber, N.; Doki, Y.; Han, E.K.; Sgambato, A.; Zhou, P.; Kim, N.-H.; Delohery, T.; Klein, M.G.; Holt, P.R.; Weinstein, I.B. Antisense to cyclin D1 inhibits the growth and tumorigenicity of human colon cancer cells. *Cancer Res.* **1997**, *57*, 1569–1574. [[PubMed](#)]
35. Zhou, P.; Jiang, W.; Zhang, Y.; Kahn, S.M.; Schieren, I.; Santella, R.M.; Weinstein, I.B. Antisense to cyclin D1 inhibits growth and reverses the transformed phenotype of human esophageal cancer cells. *Oncogene* **1995**, *11*, 571–580. [[PubMed](#)]
36. Kornmann, M.; Danenberg, K.D.; Arber, N.; Beger, H.G.; Danenberg, P.V.; Korc, M. Inhibition of cyclin D1 expression in human pancreatic cancer cells is associated with increased chemosensitivity and decreased expression of multiple chemoresistance genes. *Cancer Res.* **1999**, *59*, 3505–3511.
37. Carroll, J.S.; Prall, O.W.; Musgrove, E.A.; Sutherland, R.L. A pure estrogen antagonist inhibits cyclin E-Cdk2 activity in MCF-7 breast cancer cells and induces accumulation of p130-E2F4 complexes characteristic of quiescence. *J. Biol. Chem.* **2000**, *275*, 38221–38229. [[CrossRef](#)]
38. Li, K.; Lin, S.-Y.; Brunicardi, F.C.; Seu, P. Use of RNA Interference to Target Cyclin E-overexpressing Hepatocellular Carcinoma. *Cancer Res.* **2003**, *63*, 3593–3597.
39. Carlson, B.A.; Dubay, M.M.; Sausville, E.A.; Brizuela, L.; Worland, P.J. Flavopiridol induces G1 arrest with inhibition of cyclin-dependent kinase (CDK) 2 and CDK4 in human breast carcinoma cells. *Cancer Res.* **1996**, *56*, 2973–2978.
40. McClue, S.J.; Blake, D.; Clarke, R.; Cowan, A.; Cummings, L.; Fischer, P.M.; MacKenzie, M.; Melville, J.; Stewart, K.; Wang, S. In vitro and in vivo antitumor properties of the cyclin dependent kinase inhibitor CYC202 (R-roscovitine). *Int. J. Cancer* **2002**, *102*, 463–468. [[CrossRef](#)]
41. Sayeed, A.; Konduri, S.; Liu, W.; Bansal, S.; Li, F.; Das, G.M. Estrogen Receptor Inhibits p53-Mediated Transcriptional Repression: Implications for the Regulation of Apoptosis. *Cancer Res.* **2007**, *67*, 7746–7755. [[CrossRef](#)]
42. Bailey, S.T.; Shin, H.; Westerling, T.; Liu, X.S.; Brown, M. Estrogen receptor prevents p53-dependent apoptosis in breast cancer. *Proc. Natl. Acad. Sci. USA* **2012**, *109*, 18060–18065. [[CrossRef](#)]



43. El-Deiry, W.S.; Tokino, T.; Velculescu, V.E.; Levy, D.B.; Parsons, R.; Trent, J.M.; Lin, D.; Mercer, W.E.; Kinzler, K.W.; Vogelstein, B. WAF1, a potential mediator of p53 tumor suppression. *Cell* **1993**, *75*, 817–825. [[CrossRef](#)]
44. Li, R.; Waga, S.; Hannon, G.J.; Beach, D.; Stillman, B. Differential effects by the p21 CDK inhibitor on PCNA-dependent DNA replication and repair. *Nature* **1994**, *371*, 534–537. [[CrossRef](#)] [[PubMed](#)]
45. Huang, H.; Tindall, D.J. Dynamic FoxO transcription factors. *J. Cell Sci.* **2007**, *120*, 2479–2487. [[CrossRef](#)] [[PubMed](#)]
46. Huang, C.-Y.; Chan, C.-Y.; Chou, I.T.; Lien, C.-H.; Hung, H.-C.; Lee, M.-F. Quercetin induces growth arrest through activation of FOXO1 transcription factor in EGFR-overexpressing oral cancer cells. *J. Nutr. Biochem.* **2013**, *24*, 1596–1603. [[CrossRef](#)] [[PubMed](#)]
47. Zhu, X.; Song, X.; Xie, K.; Zhang, X.; He, W.; Liu, F. Osthole induces apoptosis and suppresses proliferation via the PI3K/Akt pathway in intrahepatic cholangiocarcinoma. *Int. J. Mol. Med.* **2017**, *40*, 1143–1151. [[CrossRef](#)] [[PubMed](#)]
48. Chao, X.; Zhou, X.; Zheng, G.; Dong, C.; Zhang, W.; Song, X.; Jin, T. Osthole induces G2/M cell cycle arrest and apoptosis in human hepatocellular carcinoma HepG2 cells. *Pharm. Biol.* **2014**, *52*, 544–550. [[CrossRef](#)]
49. Renault, T.T.; Floros, K.V.; Chipuk, J.E. BAK/BAX activation and cytochrome c release assays using isolated mitochondria. *Methods* **2013**, *61*, 146–155. [[CrossRef](#)]
50. Eldeeb, M.A.; Fahlman, R.P.; Esmaili, M.; Ragheb, M.A. Regulating Apoptosis by Degradation: The N-End Rule-Mediated Regulation of Apoptotic Proteolytic Fragments in Mammalian Cells. *Int. J. Mol. Sci.* **2018**, *19*, 3414. [[CrossRef](#)]
51. Varshavsky, A. The N-end rule and regulation of apoptosis. *Nat. Cell Biol.* **2003**, *5*, 373–376. [[CrossRef](#)]
52. Eldeeb, M.A.; Ragheb, M.A.; Fon, E.A. Cell Death: N-degrons Fine-Tune Pyroptotic Cell Demise. *Curr. Biol.* **2019**, *29*, R588–R591. [[CrossRef](#)]
53. Berridge, M.J.; Bootman, M.D.; Roderick, H.L. Calcium signalling: Dynamics, homeostasis and remodelling. *Nat. Rev. Mol. Cell Biol.* **2003**, *4*, 517–529. [[CrossRef](#)]
54. Orrenius, S.; Zhivotovsky, B.; Nicotera, P. Calcium: Regulation of cell death: The calcium–apoptosis link. *Nat. Rev. Mol. Cell Biol.* **2003**, *4*, 552–565. [[CrossRef](#)]
55. Zheng, S.; Ma, Y.; Guo, Y.; Wang, L.; Pan, Y. Osthole promote differentiation and inhibit proliferation of osteoblast by activating wnt signaling and endoplasmic reticulum stress. *Pharmacogn. Mag.* **2018**, *14*, 641–646. [[CrossRef](#)]
56. Evan, G.I.; Vousden, K.H. Proliferation, cell cycle and apoptosis in cancer. *Nature* **2001**, *411*, 342–348. [[CrossRef](#)]
57. Saini, K.S.; Loi, S.; de Azambuja, E.; Metzger-Filho, O.; Saini, M.L.; Ignatiadis, M.; Dancey, J.E.; Piccart-Gebhart, M.J. Targeting the PI3K/AKT/mTOR and Raf/MEK/ERK pathways in the treatment of breast cancer. *Cancer Treat. Rev.* **2013**, *39*, 935–946. [[CrossRef](#)]
58. Steelman, L.; Abrams, S.; Whelan, J.; Bertrand, F.; Ludwig, D.; Bäsecke, J.; Libra, M.; Stivala, F.; Milella, M.; Tafuri, A. Contributions of the Raf/MEK/ERK, PI3K/PTEN/Akt/mTOR and Jak/STAT pathways to leukemia. *Leukemia* **2008**, *22*, 686–707. [[CrossRef](#)]
59. Slamon, D.J.; Clark, G.M.; Wong, S.G.; Levin, W.J.; Ullrich, A.; McGuire, W.L. Human breast cancer: Correlation of relapse and survival with amplification of the HER-2/neu oncogene. *Science* **1987**, *235*, 177–182. [[CrossRef](#)]
60. Lin, V.C.-H.; Chou, C.-H.; Lin, Y.-C.; Lin, J.-N.; Yu, C.-C.; Tang, C.-H.; Lin, H.-Y.; Way, T.-D. Osthole Suppresses Fatty Acid Synthase Expression in HER2-Overexpressing Breast Cancer Cells through Modulating Akt/mTOR Pathway. *J. Agric. Food Chem.* **2010**, *58*, 4786–4793. [[CrossRef](#)]
61. Ding, D.; Wei, S.; Song, Y.; Li, L.; Du, G.; Zhan, H.; Cao, Y. Osthole Exhibits Anti-Cancer Property in Rat Glioma Cells Through Inhibiting PI3K/Akt and MAPK Signaling Pathways. *Cell. Physiol. Biochem.* **2013**, *32*, 1751–1760. [[CrossRef](#)]
62. Hay, N. The Akt-mTOR tango and its relevance to cancer. *Cancer Cell* **2005**, *8*, 179–183. [[CrossRef](#)]
63. Nogueira, V.; Park, Y.; Chen, C.-C.; Xu, P.-Z.; Chen, M.-L.; Tonic, I.; Unterman, T.; Hay, N. Akt Determines Replicative Senescence and Oxidative or Oncogenic Premature Senescence and Sensitizes Cells to Oxidative Apoptosis. *Cancer Cell* **2008**, *14*, 458–470. [[CrossRef](#)]
64. Cagnol, S.; Chambard, J.-C. ERK and cell death: Mechanisms of ERK-induced cell death—Apoptosis, autophagy and senescence. *FEBS J.* **2010**, *277*, 2–21. [[CrossRef](#)]

65. Zhou, Q.-M.; Wang, S.; Zhang, H.; Lu, Y.-Y.; Wang, X.-F.; Motoo, Y.; Su, S.-B. The combination of baicalin and baicalein enhances apoptosis via the ERK/p38 MAPK pathway in human breast cancer cells. *Acta Pharmacol. Sin.* **2009**, *30*, 1648–1658. [[CrossRef](#)]
66. Yeh, P.Y.; Chuang, S.-E.; Yeh, K.-H.; Song, Y.C.; Chang, L.L.-Y.; Cheng, A.-L. Phosphorylation of p53 on Thr55 by ERK2 is necessary for doxorubicin-induced p53 activation and cell death. *Oncogene* **2004**, *23*, 3580–3588. [[CrossRef](#)]
67. Dhanasekaran, D.N.; Reddy, E.P. JNK signaling in apoptosis. *Oncogene* **2008**, *27*, 6245–6251. [[CrossRef](#)]
68. Park, S.K.; Sanders, B.G.; Kline, K. Tocotrienols induce apoptosis in breast cancer cell lines via an endoplasmic reticulum stress-dependent increase in extrinsic death receptor signaling. *Breast Cancer Res. Treat.* **2010**, *124*, 361–375. [[CrossRef](#)]
69. Deng, Y.T.; Huang, H.C.; Lin, J.K. Rotenone induces apoptosis in MCF-7 human breast cancer cell-mediated ROS through JNK and p38 signaling. *Mol. Carcinog.* **2010**, *49*, 141–151. [[CrossRef](#)]
70. Alanazi, I.O.; Khan, Z. Endocrine and Cell Surface Receptor Signaling in Breast Carcinogenesis. In *Breast Cancer and Surgery*; IntechOpen: London, UK, 2018.
71. Dai, X.; Li, T.; Bai, Z.; Yang, Y.; Liu, X.; Zhan, J.; Shi, B. Breast cancer intrinsic subtype classification, clinical use and future trends. *Am. J. Cancer Res.* **2015**, *5*, 2929–2943.



© 2019 by the authors. Licensee MDPI, Basel, Switzerland. This article is an open access article distributed under the terms and conditions of the Creative Commons Attribution (CC BY) license (<http://creativecommons.org/licenses/by/4.0/>).